A review of the standardized measurement of the characteristics of graphene-based materials

Zhang Donghui[1,*], Li Wan[1], Ou Bingxian[2], Wang Liangwang[3], Ge Guanglu[1,*]

(1. *CAS Key Laboratory of Standardization and Measurement for Nanotechnology, National Center for Nanoscience and Technology, Beijing* 100190, *China*;
2. *National Graphene Products Quality Inspection and Testing Center (Jiangsu), Special Equipment Safety Supervision Inspection Institute of Jiangsu Province, Wuxi* 214174, *China*;
3. *National Quality Inspection and Testing Center of Graphene Products (Guangdong), Guangzhou Academy of Special Equipment Inspection & Testing, Guangzhou* 510030, *China*)

Abstract: Standardization is necessary for the early industrialization of the new materials and technology. It is achieved by having agreed practices for the measurement of properties and other characteristics. The promising use of graphene-based materials in fields like electronics, energy, and composites has resulted in standards for their nomenclature, the measurement of key characteristics, and their specification, etc. Among these, standards for measuring the key characteristics are crucial. The critical parameters are the number of layers, the type and concentration of defects and functional groups, elemental composition, sheet resistance, and carrier mobility. Standards for characterizing these have been analyzed by the International Organization for Standardization Technical Committee in ISO/TC229 and the International Electrotechnical Commission Technical Committee in IEC/TC113. These give details of applicable or preferred samples, the fundamental principles of the techniques, specific precautions, and points for attention in the relevant standards. The pivotal role of the ISO/TC229 and IEC/TC113 standards is considered and challenges and future trends are outlined.

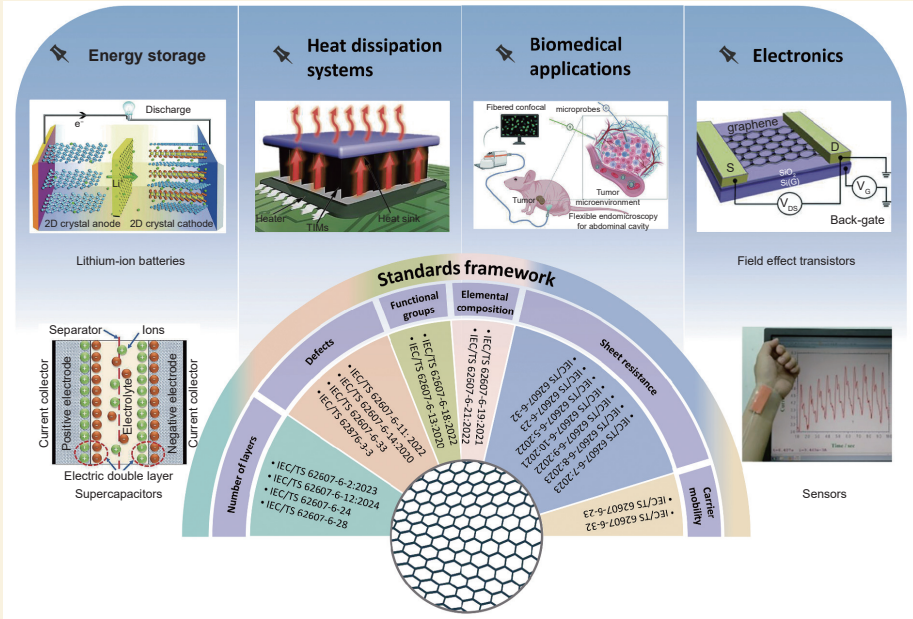

Key words: Nanotechnology; Graphene-based materials; Measurement standards; Critical characteristics; Quality control

1 Introduction

Graphene has revolutionized materials science by driving breakthroughs and promising applications across different areas because of its extraordinary properties[1–3]. Electronics and wearable device, photonics, biomedical, and energy storage are examples of important graphene-base materials (GBMs) applications[4–5]. Interests in its commercialization increased explosively. Intensive efforts have been made to use graphene in commercial products. It is estimated that the production of GBMs in 2023 was as high

Received: June 30, 2025
Revised: September 11, 2025
Accepted: September 12, 2025

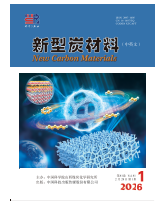

as 1.6×10^9 kg. However, a global survey of 60 graphene samples by adopting well-defined protocol as benchmark revealed critical quality issues[6]. Significantly disparate data in all the measured characteristics indicate information solely provided by the supplier is not convincing or potentially misleading. On one hand, confusion and misinformation are caused by lack of comparability of data originated from different laboratories and producers[6–7]. On the other hand, inconsistency arises from different techniques and/or parameters may adopted for measuring the same characteristic. To facilitate market acceptance, clear and widely accepted standards including detailed measurement protocols for characterizing various graphene-based materials is highly desired. Boggild emphasized that standards are essential for GBMs to leave the starting block in dozens of applications[8]. As a matter of fact, quality metrics and assurance system are imperative for any new materials to be accepted by the market and adopted to industry. It is especially true for GBMs because they are plentiful in physical forms, structure, properties and applications.

Extensive reviews have been published centered on the graphene synthesis, characterization methodologies, and application scenarios[9–11]. However, comprehensive reviews addressing graphene research from the perspective of measurement standardization are notably scarce. Alves et al. reviewed techniques, such as ultraviolet–visible spectroscopy, Raman spectroscopy, X-ray photoelectron spectroscopy, X-ray diffraction, etc., for characterizing graphene, based on what have been reported by literature and standards[12]. Pollard described the advances in the structural and chemical characterization of graphene, and highlighted that standardization will significantly aid global graphene applications[13].

Standards are good practices based on scientifically accepted techniques reported in the literature and industry practices. Measurement standards include specified characteristics and measurands, as well as the applicable measurement methods and procedures. They provide unified criteria for determining the quantity and quality of GBMs. This makes reliable, reproducible and accurate comparisons for GBMs among different parties (buyers, sellers, academics, regulatory bodies, third-party organization, etc.) possible. Parameters in the measurement procedures, including sample preparation, measurement conditions, data analysis, and uncertainty assessment are settled through stakeholder's consensus after intensive discussion. Measurement standards accelerate the development of graphene technology and industry in multiple ways. Standardized protocols create a consistent framework for characterizing GBMs, ensuring rigorous quality control during R&D. Producers maintain uniform material quality via these metrics, fostering reliable performance and market trust. Clear standards enable users to differentiate products and make informed decisions based on reliable data. Uniform criteria reduce uncertainties in technology transfer, bridging academic innovation and industrial manufacturing to expedite commercialization. Standards also allow systematic comparison of materials from different suppliers, giving buyers a trustworthy basis for evaluation. These factors collectively underscore the pivotal role of standardization in scaling GBMs applications.

This review summarizes the current progress in measurement standards for six critical characteristics of GBMs, as developed by ISO/TC229 (International Organization for Standardization/Technical Committee 229) and IEC/TC113 (International Electrotechnical Commission/Technical Committee 113) (Fig. 1). The six characteristics —number of layers, defects, functional groups, elemental composition, sheet resistance, and carrier mobility—are systematically linked to corresponding international standards. This approach enables stakeholders to efficiently identify relevant standards aligned with specific application needs. The main text is structured into six sections focusing on these characterization parameters, allowing readers to quickly access customized protocols. The concluding section highlights current challenges and emerging trends in GBMs standardization. Through this comprehensive analysis, we anticipate broader adoption of these standards across industries, facilitat-

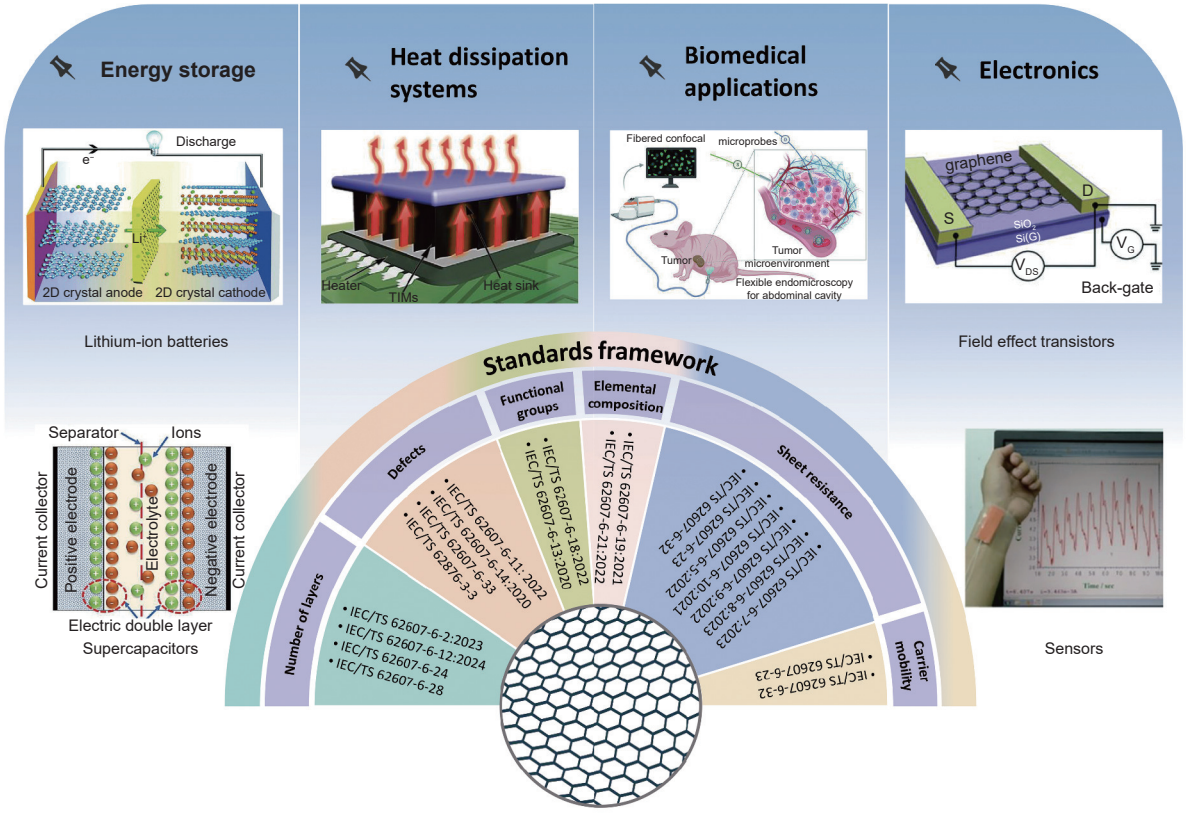

Fig. 1 Schematic diagram of the topics covered in this review[16–21]. (Reproduced with permission)

ing their practical implementation.

Six key characteristics were selected based on their representation in international standards. These standards reflect both industrial priority needs and validated relevance in scientific publications. ISO/TC229 has established key frameworks through ISO/TR 19733:2019 and ISO/TS 21356-1:2021, introducing a standardized matrix for property-measurement correlation and a systematic strategy for structural characterization of GBMs[14–15]. In parallel, IEC/TC113 developed the IEC/TS 62607 series, which comprise 22 published and 14 under-development standards. Standard addressing electronic properties, including sheet resistance and carrier mobility, account for the largest proportion (33.3%), followed by those related to layer number (11.1%) and defect (8.3%), with functional group (5.6%) and elemental composition (5.6%) followed in subsequent order. Such prioritization in standard development underscores these six characteristics' high industrial significance and established technical relevance across research fields.

2 Number of layer

The number of graphene layers is crucial as it directly influences the mechanical, thermal, and electrical properties and performance[22]. This directly influences the application of GBMs across multiple fields. For instance, in energy storage, fewer-layered graphene exhibits higher electrical conductivity and ion transport efficiency, thereby enhancing energy and power density in lithium-ion batteries[23]. Similarly, in photoelectrochemical systems, optical transparency decreases as layer increase from 1 to 7, reducing photoanode efficiency[24]. Thus, precise characterization of layer number is essential to optimize performance in these applications.

Several measurement standards have been developed for graphene layer determination based on more than one technique (Fig. 2)[25–26]. IEC/TS 62607-6-2:2023 and IEC/TS 62607-6-12:2024 have been specifically designed to ensure accurate determination of layer numbers[27–28]. IEC/TS 62607-6-2:2023 employs an analytical approach combining AFM, op-

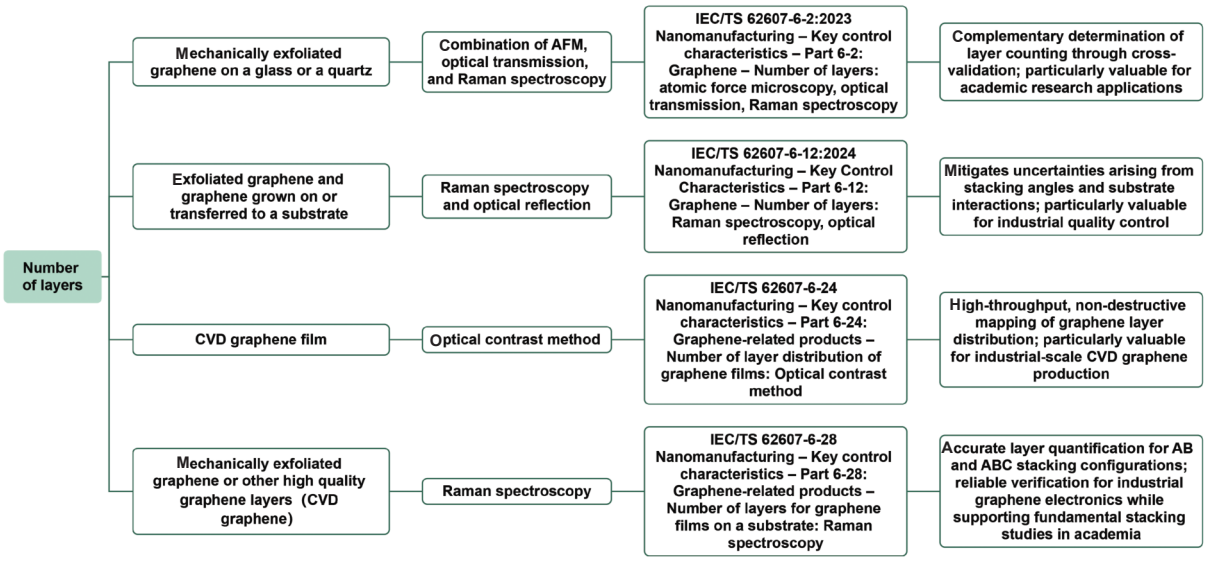

Fig. 2 Brief summary of standards for number of layers

tical transmission, and Raman spectroscopy for mechanically exfoliated graphene with 1-10 layers, achieving enhanced precision through cross-validation of these complementary measurement modalities. A flow chart shown in Fig. 3a illustrates these process as follows: Raman spectroscopy is initially employed for a preliminary assessment of layer number, based on the position and intensity ratio of the *G* peak and 2*D* peak. Subsequently, AFM topography analysis uses the thickness data which have been adjusted for offset height to infer the layer number. Finally, reflectance analysis serves as a supplementary step. For this method, calibration procedures are a critical prerequisite for ensuring measurement accuracy across AFM, Raman spectroscopy, and optical reflectance characterization platforms. This is particularly true for AFM test, which exhibits high sensitivity to the substrate and environment. However, this prerequisite and instrument combination inevitably diminishes its versatility and user friendliness to some extent. It should be noted that interaction among the substrate, the probe, and the sample may cause inconsistent results from Raman spectroscopy and AFM.

IEC/TS 62607-6-12:2024 targets graphene films on glass or 90 nm SiO_2/Si substrates with low defect density, low surface contamination, and fewer than 5 layers, using Raman spectroscopy and optical contrast measurement[27]. To accurately determine graphene layer number, the standard addresses challenges from stacking angles and substrate interactions by correlating *G*-peak integrated intensity (normalized to a highly oriented pyrolytic graphite) with optical contrast (substrate-dependent reflectance difference). This method enables the precise layer counting despite complex material interactions. As shown in Fig. 3b, Ni et al. quantified optical contrast on a 285 nm SiO_2/Si substrate[29], observing distinct contrast spectra and optical images for 1–10 graphene layers. The intensity increases progressively within 10 layers and negative contrast emerging beyond 10 layers. The authors derived an empirical equation for layers up to 10 layers based on these observations. Notably, the optical reflection principle they demonstrated was later adopted in IEC/TS 62607-6-12. Supplementing IEC/TS 62607-6-2:2023, this standard applies to exfoliated graphene and graphene grown/transferred to glass or oxidized silicon substrates. However, the measurement area is limited by the laser spot size, and calibration process using Raman reference sample and reflection reference sample is perquisite for the measurement.

An alternative standard is currently being developed to quantitatively characterize both layer number and layer number distribution[30]. IEC 62607-6-24 establishes a high-throughput and non-destructive measurement approach for chemical vapor deposition

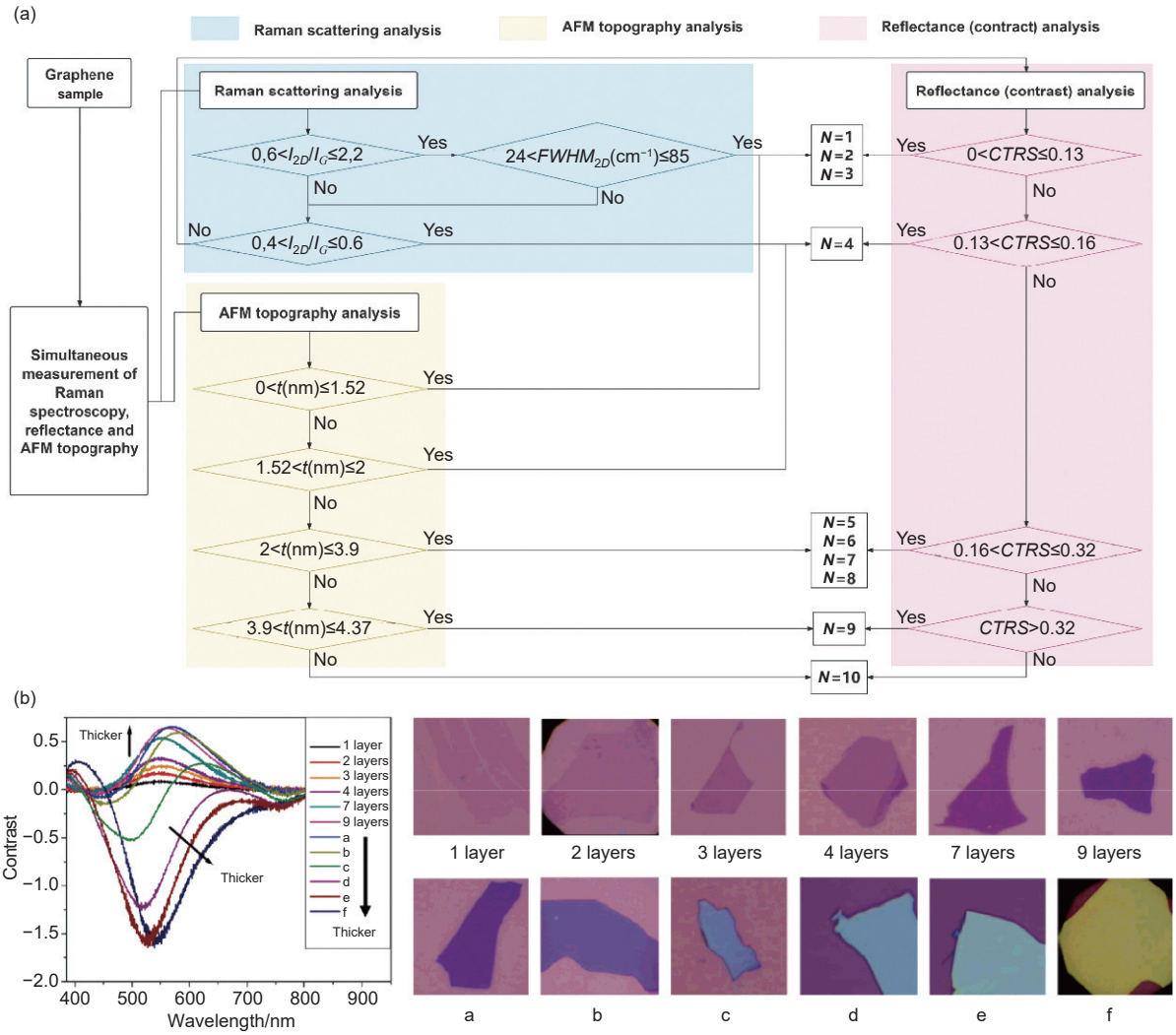

Fig. 3 (a) Flowchart for determining the number of layers of graphene in IEC/TS 62607-6-2:2023[28]. (b) The contrast spectra of graphene sheets with different thicknesses, together with the optical image of all the samples[29]. (Reproduced with permission)

(CVD) graphene film by optical contrast analysis. The principle relies on the variations in green channel contrast values (520–590 nm), comparing contrast between a blank substrate (e.g., 300 nm SiO_2/Si) and graphene films with different layer numbers. With light corrections, accurate coverage ratio of mono- and multilayer domains in large-scale CVD graphene can be obtained. Enabled by large-area optical contrast measurement, this standard outperforms others by providing both layer number and layer number distribution for graphene film. This represents a significant advancement over single-point layer number measurement. Moreover, it requires no sophisticated instruments. A simple white balance calibration using a standard whiteboard under the objective lens suffices. These features make it suitable for high-throughput, rapid industrial inspection, enabling efficient uniformity assessment of graphene film though the standard excludes the twisted or complex multilayer structures.

IEC/TS 62607-6-28, which is proposed almost at the same time as IEC/TS 62607-6-24, dedicates to the assessment of layer number of graphene prepared by mechanical exfoliation and other high quality graphene layers[31]. Two complementary protocols based on Raman spectroscopy are thoroughly explained. Protocol A analyzes the line shape of the 2D peak under 633 nm laser excitation. It enables the determination of AB-stacked graphene layers, with applicability up to 4 layers. Spectral features are dir-

ectly compared to references, for example, 2599 cm^{-1} for bilayer graphene. However, this protocol becomes less reliable with more layers due to peak overlap. Protocol B measures the silicon substrate intensity ratio under 532 nm excitation. This approach extends detection capabilities to 10 layers for both AB and ABC stacking. Subsequently, the measured value is compared with theoretical values in reference tables to precisely assign the layer number. Since the thickness of SiO_2 of an oxidized silicon substrate and the numerical aperture of the microscope objective both critically impact the results. Thus, strict control of these two parameters during measurement is essential. In brief, this standard supports both AB and ABC stacking, making it highly recommended for graphene commercial transaction. Its accuracy in layer quantification provides reliable verification, which is critical in resolving trade disputes.

Successive standards for layer number determination reflect the field's evolving research advancements: IEC/TS 62607-6-2:2023 and IEC/TS 62607-6-12:2024 adopt multi-technique combinations, while IEC 62607-6-24 and IEC 62607-6-28 (under development) use simplified single-technique protocols. This methodological shift from multi-instrument validation to simplified, application-driven protocols highlights alignment with both scientific innovation and industrial demands. It further illustrates how foundational research and standardization adapt to industry needs.

3 Defect

Defect is another key characteristic that could remarkably influence the mechanical, electronic, and optical properties and thus applications of graphene. On one hand, the presence of defects can decrease the mechanical strength and carrier mobility of graphene, which is critical for high-performance electronic, optoelectronic and electrochemical devices[32]. On the other hand, strategic introduction of defects, including heteroatom doping and vacancy creation, can optimize the structure and physicochemical properties of materials, thereby enhancing the electrochemical performance of two-dimensional (2D) materials[33]. For instance, defects can provide additional active sites, facilitate ion diffusion, boost power density, and improve stability, and these enhancements significantly contribute to improving the performance of energy storage devices such as metal-ion batteries and fuel cells[33–35].

Usually, defects in graphene films (Fig. 4a and 4b) are characterized by the intensity ratio of several peaks, the principle 2*D* and *G* peaks, as well as defect activated *D*, *D*' and *D*+*D*' peaks, in Raman spectra (Fig. 4c)[36]. Two standards, IEC/TS 62607-6-11:2022 and IEC/TS 62607-6-14:2020, have been developed successively to measure defect in GBMs to address evolving needs in the field (Fig. 5)[37–38]. Both standards utilize Raman spectroscopy as the core technique, but they target different sample types (film vs. powder) and application scenarios (electronic applications vs. industrial quality control). IEC/TS 62607-6-11:2022 focused on high-precision defect density analysis in graphene films for electronic applications. This requires complex doping corrections to ensure accuracy. In contrast, IEC/TS 62607-6-14:2020 prioritizes rapid defect assessment in powders for industrial quality control. It sacrifices the detailed characterization for operational simplicity.

Specifically, IEC/TS 62607-6-11:2022 covers CVD grown films and mechanically exfoliated mono/few-layer graphene requiring no sample preparation. It quantifies defect density (n_D) through the Raman intensity ratio of the defect-activated *D* peak to the *G* peak (I_D/I_G). It specifies a micro-Raman spectrometer with laser power density below 1.27 $mW/\mu m^2$ (514 nm or 532 nm excitation for optimal resolution) to prevent thermal damage. Applicable defects range is from 2.46×10^{10} to 7.39×10^{11} cm^{-2} under 2.41 eV (514 nm) excitation. Notably, doping sensitivity necessitates formula corrections during analysis. This standard classifies graphene lattice disorder in a three-stage framework (from graphite to amorphous carbons) aiding Raman spectra interpretation. It also provides sampling guidance for circular/rectangular/irregular substrates to ensure whole wafer quality

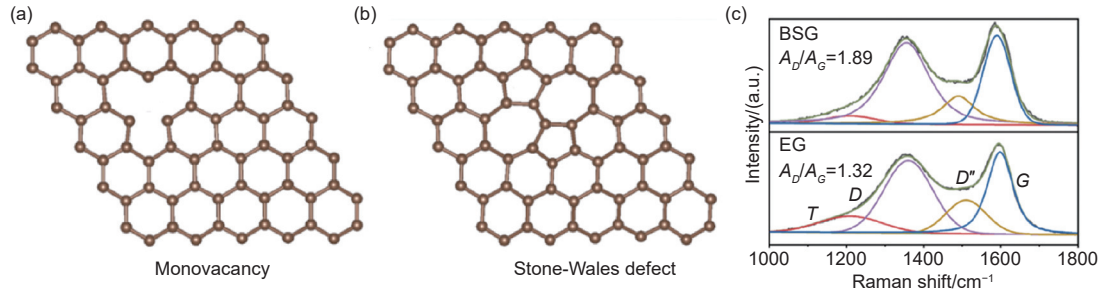

Fig. 4 DFT computational models of (a) monovacancy and (b) Stone-Wales defects. (c) Raman spectra of novel graphene blocks and expanded graphene[36]. (Reproduced with permission)

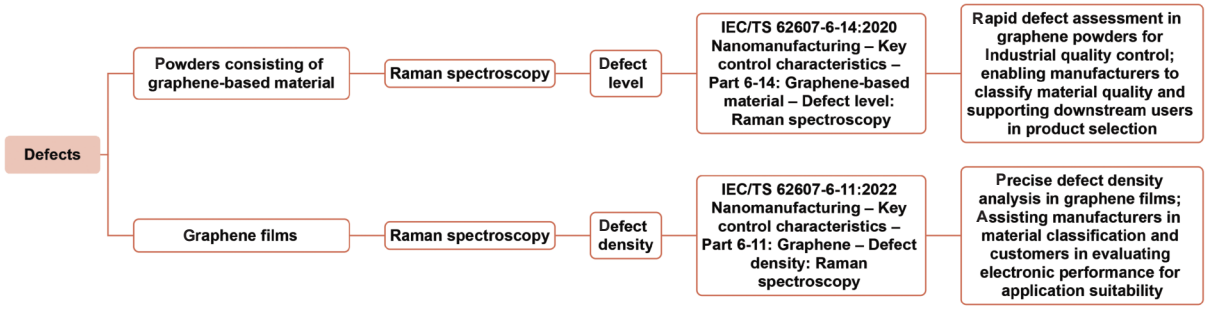

Fig. 5 Brief summary of standards for defects

characterization. Cancado et al. validated the I_D/I_G ratio and *G*-band broadening for defect metrology, aligning with this standard's framework. Tip-enhanced Raman spectroscopy (TERS), with nanoscale resolution, is expected complements micro-Raman methods for 2D material defect mapping[39]. IEC/TS 62607-6-14:2020 focuses on assessing powder (e.g., reduced graphene oxide (rGO), multilayer graphene powders) defect level through the $I_{D+D'}/I_{2D}$ ratio[37]. Powder samples edges/boundary abundance necessitates this ratio to minimize signal interference. Samples should be pressed into thick tablets to eliminate substrate signals. The confocal Raman spectrometer should be capable of laser power density of 0.4–1.2 mW/μm^2 with 532 nm excitation wavelength for optimal resolution. The method is inapplicable to highly defective samples as 2D peak may become undetectable when defect levels exceed threshold. Additionally, it can not distinguish defect types (e.g., Stone-Wales defects, vacancies, or edge/boundary states) due to overlapping Raman signatures in the *D*-peak region.

New standard is under active development to advance defect characterization in graphene-based materials: IEC/TS 62607-6-33 Nanomanufacturing – Key control characteristics – Part 6-33: Graphene – Defect density: Electron Energy Loss Spectroscopy (EELS). IEC/TS 62607-6-33 specifies the use of EELS, which overcomes the limitations of Raman spectroscopy in differentiating defect types. This is achieved by providing atomic-scale chemical bonding information and electronic state identification[40]. Similarly, scanning tunneling microscopy (STM) technique offers atomistic structure of 2D materials and identifies the topological defects, making it another powerful tool for characterizing defects and a promising candidate for future standardization[41].

4 Functional group

The introduction of functional groups provides essential insights into the chemical structure and reactivity of GBMs, which directly influence their physical and chemical properties, thereby altering their electronic, mechanical, and chemical behaviors[42]. For instance, the presence and distribution of oxygen-containing functional groups on graphene oxide (GO) greatly affect its hydrophilicity, electronic structure, and catalytic activity[43]. Additionally, understanding

the composition and concentration of functional-groups allows for the precise tuning of properties for-specific applications (Fig. 6).

IEC/TS 62607-6-18:2022 outlines a standard to comprehensively determine multiple functional groups of functionalized GBMs[44]. It employs a thermogravimetry analysis (TGA) coupled with FTIR. This TGA-FTIR system combines TGA for mass change tracking and FTIR for evolved gas analysis (Fig. 7a). Specifically, the sample is heated at a given heating rate from room temperature to the desired temperature in an inert gas. The mass changes from sample pyrolysis and vaporization that accompany changes in temperature are measured quantitatively by the TGA. Qualitative analysis of the evolved gases from pyrolyzed materials can be monitored simultaneously by FTIR measurement. The tablet sample with mass at least 5 mg is utilized. After the measurement TGA curve and three-dimensional (3D) FTIR spectrum can be obtained. Due to the inherent trait of the

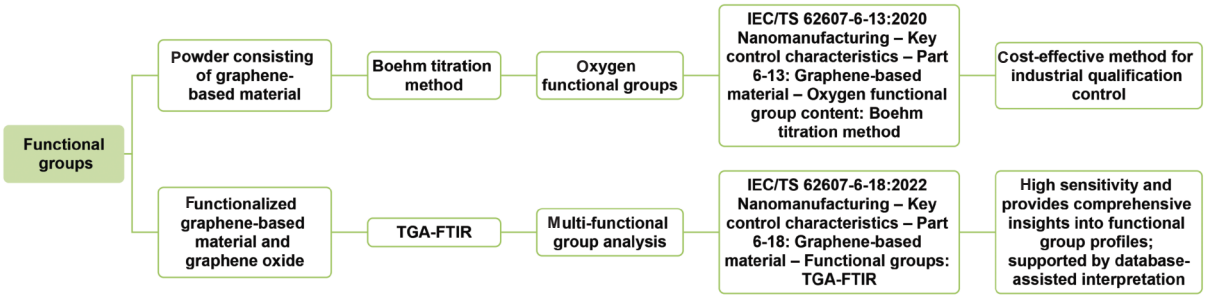

Fig. 6 Brief summary of standards for functional groups

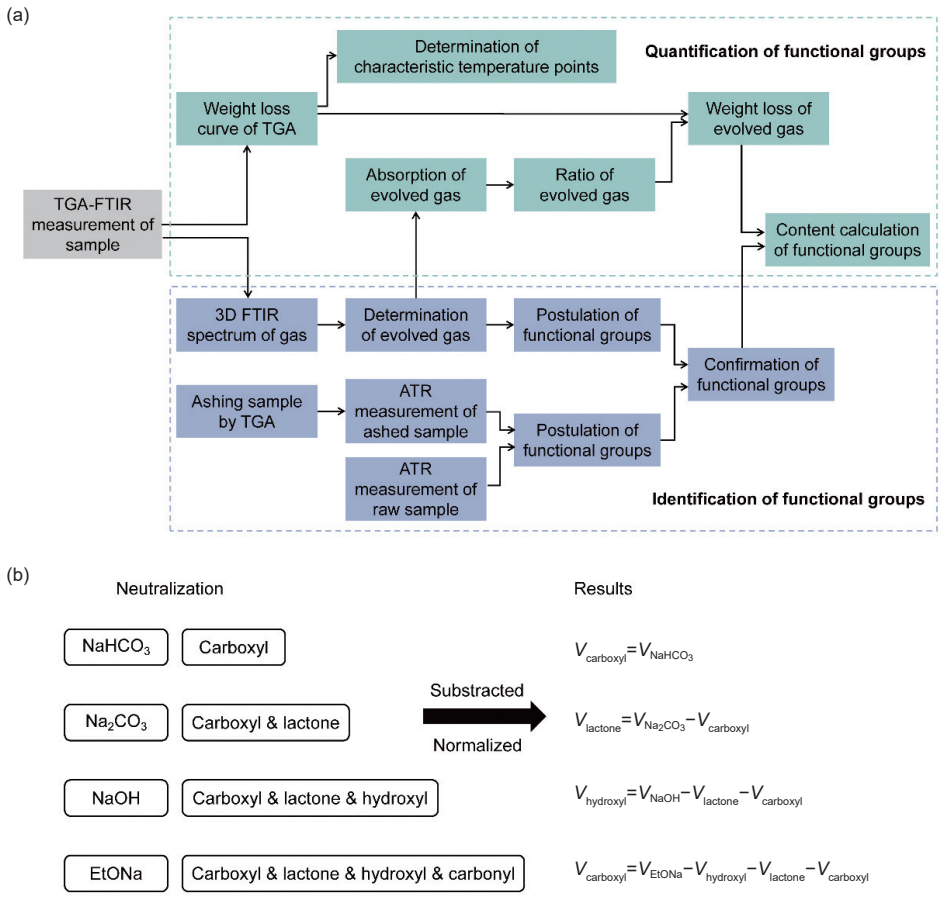

Fig. 7 (a) Flowchart for TGA-FTIR analysis in IEC TS 62607-6-18 (b) Principle of Boehm titration in IEC TS 62607-6-13[44–45]

hyphenated TGA-FTIR technique, this method is expected to demonstrate high sensitivity and offers insights into broad functional group profiles. However, the complexity of spectral deconvolution necessitates skilled interpretation, which is often supported by databases (e.g., Wiley KnowItAll FTIR Database).

IEC/TS 62607-6-13:2020 standardize the Boehm titration method to determine the oxygen functional groups content on GBMs[45]. This standard utilizes bases with varying strengths (e.g., sodium bicarbonate, sodium carbonate, sodium hydroxide, and sodium ethoxide) to quantify oxygen functional groups (e.g., carboxyl, lactone, hydroxyl, and reactive carbonyl groups) by neutralization reactions. The core principle involves two steps: first, differentiating these functional groups based on their acidity; then quantifying their absolute concentrations through titration of the filtrate after filtration (Fig. 7b). This standard applies to powdered GBMs, excluding sulfonated graphene. The detection limitations are specified as follows: 0.015 mmol/g for carboxyl groups, 0.037 mmol/g for lactone groups, 0.014 mmol/g for hydroxyl and 0.072 mmol/g for carbonyl. This standard provides absolute values of the surface concentration of oxygen functional group and avoid the ambiguity and subjectivity brought by spectroscopy. It provides profiles of acidic surface oxygen functionalities, and is featured by cost-effective for industrial qualification control. Aliyev et al. successfully employed Boehm titration method to precisely quantify lactone groups in graphene oxide layers. Possible new structures for GO layers and oxidative debris were proposed based on several techniques by Aliyev et al.[46]. Complementary analytical methods have been employed in recent studies to quantify specific functional groups, such as NMR for amine- or thiol-functionalized moieties and neutron scattering for hydrogen-containing groups[47–48]. Looking ahead, standardization of these techniques is anticipated to provide users with a wider range of validated measurement protocols.

5 Elemental composition

Heteroatoms (e.g., S, O, N, H) are inevitably introduced during graphene fabrication, whether through laboratory synthesis or commercial production. These impurities modulate the material's electronic band structure, thereby influencing its electrical conductivity and thermal transport properties[49–50]. While carbon (C) forms the foundational lattice, oxygen (O), nitrogen (N), sulfur (S), chlorine (Cl), and silicon (Si) even at trace concentrations act as inherent dopants that directly impact the performance of graphene in electronic and thermal applications. Beyond elemental composition, atomic ratios such as C/O serve as critical quality metrics. The C/O ratio differentiates pristine graphene from graphene oxide (GO) and quantifies the reduction efficiency of reduced graphene oxide (rGO). Variability in production processes and suppliers introduces significant discrepancies in elemental profiles and C/O ratios. Standardized quantification of these ratios is essential for ensuring consistency in industrial applications, particularly in high-precision sectors such as microelectronics and energy storage.

Two standards have been published for quantification of elemental composition for GBMs (Fig. 8). IEC/TS 62607-6-19:2021 established a protocol to determine elemental composition for graphene powders

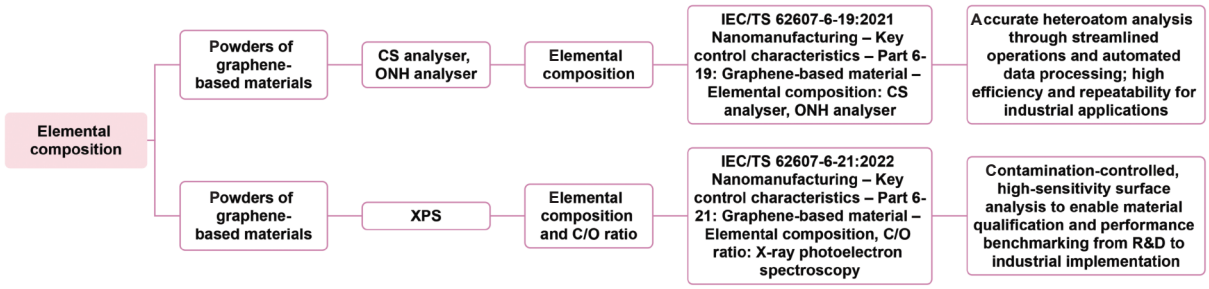

Fig. 8 Brief summary of standards for elemental composition

by CS analyzer and ONH analyzer[51]. The fundamental principle of this method is based on bulk elemental analysis by combustion/pyrolysis techniques. The carbon (C) and sulfur (S) contents in graphene powder are determined via their conversion to CO, CO_2, and SO_2. These gaseous products are then quantified by an infrared gas detector (IGD) within a CS analyzer. Meanwhile, oxygen (O), nitrogen (N) and hydrogen (H) contents in graphene powder are determined through ONH analyzer by pyrolysis. Specifically, O is converted to CO/CO_2, detected by an IGD. N is converted to N_2, measured by a thermal conductivity detector (TCD). H is converted to H_2 or H_2O, with detection by TCD (for H_2) or IGD (for H_2O). To ensure accuracy, certain details in sample preparation should be carefully noted: sufficient drying to eliminate residual moisture, sample pressing to prevent splatter during combustion, and adequate preheating of corundum crucibles to avoid interference from residual carbon. This method features user-friendly instrument operation, simplified sample preparation, and automated data analysis enabled by integrated software. These make this standard featured by high analysis efficiency and robust repeatability in heteroatom determination. Fig. 9 illustrates the measurement results of samples with low C content (Fig. 9a) and high C content (Fig. 9b) by CS analyzer.

Unlike bulk analysis techniques, IEC/TS 62607-6-21:2022 specified X-ray Photoelectron Spectroscopy (XPS) for surface-sensitive elemental composition analysis, which enables precise determination of elemental composition and the C/O ratio[52]. The elemental composition (species and relative abundance) is derived by the elemental binding energy and integral peak area at corresponding portion of XPS spectrum. Typical elements include C, O, N, S, Cl and Si. It is applicable to powders of graphene, GO, rGO, and functional derivatives. This standard provides chemical state information for elements like Cl and Si, it can not detect hydrogen due to inherent limitations of XPS. Additionally, the sample should be pressed into pellets thinner than 1 mm and placed on a silicon. The XPS-based technique enables high-sensitivity surface analysis of functionalized graphene derivatives, which requires strict contamination control.

Inductively coupled plasma mass spectrometry (ICP-MS) is a validated and widely adopted method for trace metal analysis. ISO/TS 13278:2017 estab-

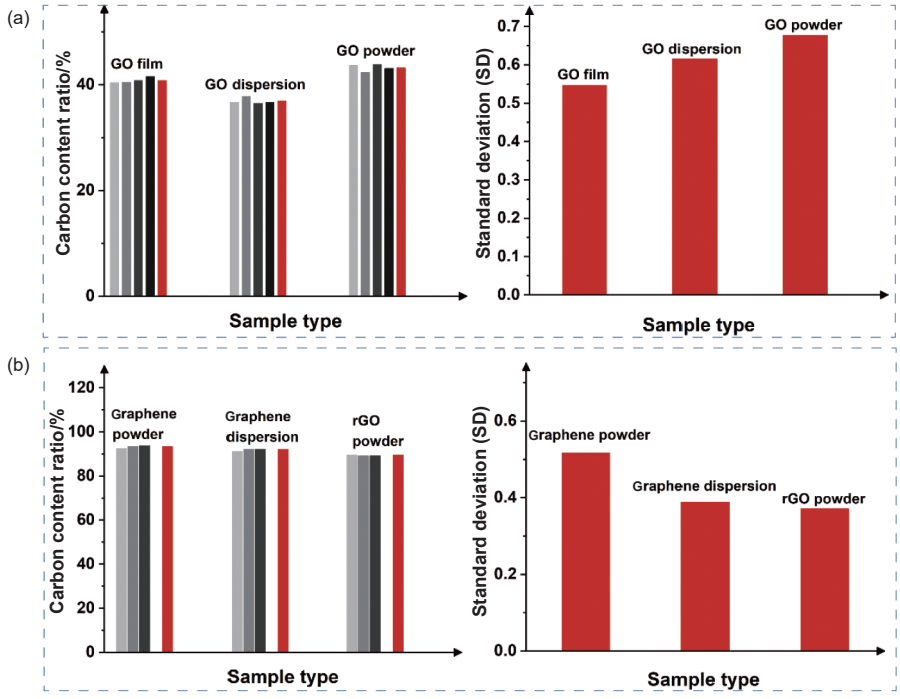

Fig. 9 Measurement results of samples with (a) low C content and (b) high C content[51]

lished specified procedures for quantifying metallic impurities in carbon nanotubes (CNTs) by ICP-MS[53], leveraging its advantages of high sensitivity, multi-element capability, and broad commercial availability. Given the structural similarities between CNTs and GBMs, the established CNT analysis framework provides a robust reference for adapting ICP-MS protocols to GBMs.

6 Sheet resistance and carrier mobility

In GBMs applications, the electronics sector stands out as the dominant domain, accounting for 27% of the market share. This highlights its pivotal role and signals significant growth opportunities in high-tech innovation[54]. Quality assessment of graphene products relies on rigorous electrical property evaluation, with sheet resistance (R_s) serving as a fundamental metric to characterize local conductivity in finite-sized graphene samples[55]. R_s, defined as the resistance between 2 opposite edges of a square thin film section, is expressed in ohms per square (Ω/sq). Single layer graphene typically shows R_s values of several hundred to several thousand Ω/sq, while few-layer graphene exhibits lower resistance (10–1000 Ω/sq)[56–57]. Moreover, precise R_s measurement is critical for ensuring performance consistency in commercial devices, meeting industry requirements, and enabling mass production scalability.

IEC/TS 62607-6-7:2023 and IEC/TS 62607-6-8:2023 each establish standardized methodologies for evaluating the sheet resistance (R_s) of graphene samples. The former uses the van der Pauw (vdP) method, while the latter applies the in-line four-point probe (4PP) method[55,58] (Fig. 10). Both documents applicable for CVD graphene on quartz substrates or other insulating materials, with a measurement range from 10^{-2} to 10^4 Ω/sq. In both vdP and 4PP methods, the sample supporting substrate should be planar and insulating to prevent any contribution to the resistance. They also share a common requirement in utilizing 4 electrodes, which are readily supported by commercial fixtures.

A fundamental distinction lies in their electrode configurations (Fig. 11). For the 4PP method, four probes are arranged in a linear, equidistant pattern directly on the sample surface, enabling precise characterization of in-plane electrical properties. When using this standard, the applied current I must be optimized: it should not damage the sample but must be sufficiently large to ensure accurate voltmeter readings (typically 1–100 μA). To enhance accuracy, each voltage measurement is performed twice with positive and negative currents of equal magnitudes. Averaging these results reduces thermoelectric effects that introduce systematic errors. In contrast, the vdP method positions electrical contacts along the sample boundary. This design avoids sample being scratched by the probes. This method calculates R_s by taking both vertical and horizontal resistances into account. In principle, it is insensitive to sample shape or contact position. However, real-world corrections are necessary because existing practical graphene samples often exhibit inhomogeneous, which can be attributed to the structural defects, non-uniform doping, or inconsistent layer thickness during synthesis and processing. Both standards require control of ambient temperature and humidity, as graphene conductivity is sensitive to these parameters. The 4PP standard (IEC/TS 62607-6-8:2023) complements the vdP approach (IEC/TS 62607-6-7:2023) when reliable placement of contacts on the sample boundary is not feasible. Scientific evidence supports that purely mechanical contacting yields reliable electrical measurements for rigid CVD graphene in both methods. For non-uniform samples, the vdP method addresses spatial variability through leveraging multi-configuration averaging[59].

For atomic-thin 2D materials, thickness is ill-defined for ultrathin (near-monolayer) films, complicating the expression of thickness-dependent electronic resistivities. Transmission line measurement (TLM) circumvents this challenge as it eliminates the need for thickness measurements in resistance calculations. IEC/TS 62607-6-5:2022 standardizes sheet resistance evaluation for 2D materials by TLM, specifying a pat-

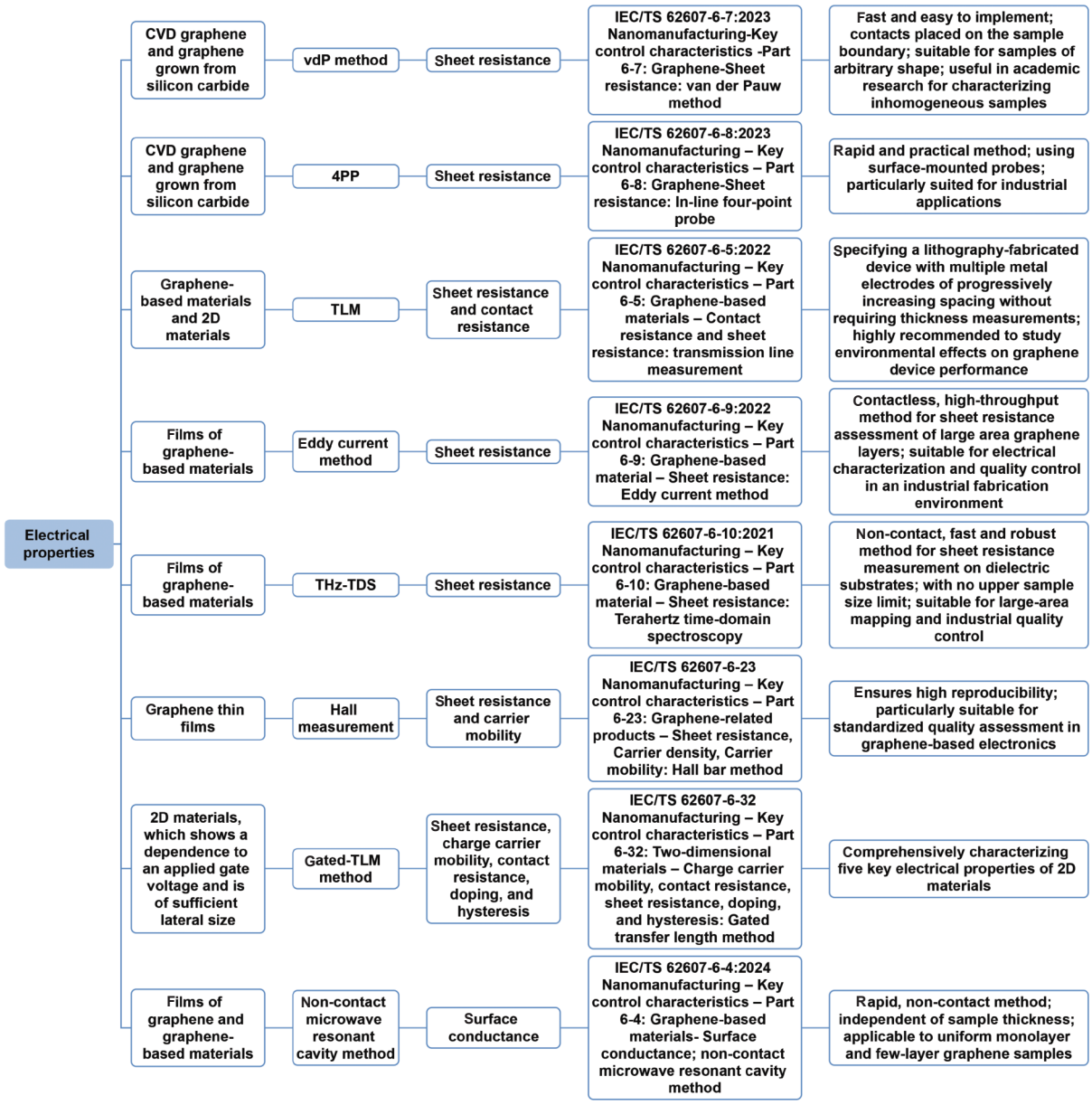

Fig. 10 Brief summary of standards for sheet resistance and carrier mobility

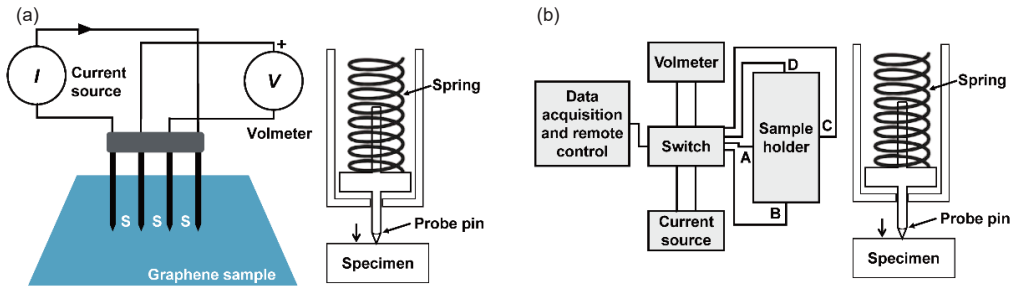

Fig. 11 (a) Schematic view of the 4PP and (b) van der Pauw measurement setup[55,58]

terned device with multiple electrode pairs of progressively increasing spacing[60]. In this standard, resistance is determined by measuring voltage across electrode pairs, requiring ohmic contact between the sample and metal electrodes. The TLM pattern is fabricated by lithography (Fig. 12). For example, a

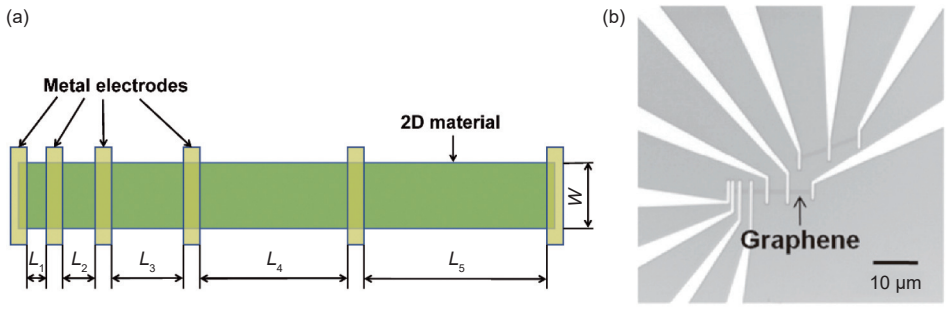

Fig. 12 (a) TLM pattern structure and (b) TLM pattern on graphene[62]. (Reproduced with permission)

graphene channel with width (W) 30 μm and length (L) from 10–50 μm (10 μm increments). Additional patterns (L = 5, 10, 15, 20 and 25 μm) are often fabricated for comparison. Channel length is optimized empirically: too short (large error) or too long (non-uniformity-induced nonlinearity) compromises data reliability. Typically defined by photolithography (similar to Field Effect Transistor fabrication), TLM patterns for small 2D samples use electron-beam lithography (EBL), involving spin-coating an electron-beam resist layer. Measurements employ a semiconductor parameter analyzer and probe station, ensuring reproducible results. Quellmalz et al. used the TLM to demonstrate that contact resistance is insensitive to humidity. However, sheet resistance is sensitive to humidity and thus requires strict control (Fig. 13a, b)[61]. This standard is highly recommended for studying the effects of environmental factors on the performance of graphene device.

Other published standards for sheet resistance include IEC/TS 62607-6-9:2022 (eddy current method) and IEC/TS 62607-6-10:2021 (terahertz time - domain spectroscopy, THz - TDS)[63–64]. Both standards describe non-contact, high-throughput methods ideal for industrial quality control and electrical properties characterization. The eddy current method evaluates samples with sheet resistance from 10 to 5000 Ω/sq, requiring continuous films without conductive overlayers. It mandates a minimum area of 25 mm×25 mm for single point measurements and 50 mm×50 mm for imaging. In contrast, the THz-TDS method has no upper size limit but requires sample transfer to dielectric substrates (e.g. quartz, silica, silicon, sapphire, silicon carbide and polymers). A newly published standards, IEC/TS 62607-6-4:2024, specifies the microwave resonant cavity technique for measuring the surface conductance in films of graphene and GBMs[65]. This method enables rapid, non-contact measurement of average sheet resistance over large-area samples, independent of sample thickness. It is particularly suitable for uniform monolayer and few-layer graphene samples[66].

Carrier mobility is another crucial parameter represents the electrical characteristics of graphene-based

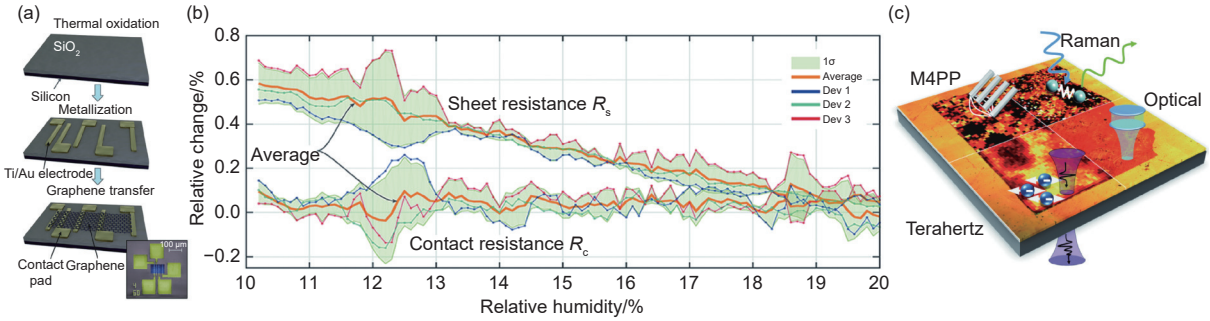

Fig. 13 (a) Schematic process flow of TLM device fabrication[61]. (b) Relative change in gold-graphene contact resistance R_c and sheet resistance R_s with relative humidity. Solid bold lines (orange) are the average of the respective data sets. The shaded areas represent one standard deviation (1σ)[61]. (c) Sketch depicting the principle of parallel mapping of electrical conductance, Raman response and optical absorption on a single-layer large area graphene film by THz-TDS, M4PP, micro Raman spectroscopy, and optical microscopy[69]. (Reproduced with permission)

materials[59]. It quantifies the speed of charge carriers (electrons/holes) under an external electric field. Two standards for carrier mobility, IEC/TS 62607-6-23 (Hall measurement) and IEC/TS 62607-6-32 (gated-TLM), are under development[67–68]. These eight IEC measurement standards (Fig. 10) address diverse scenarios for characterizing sheet resistance and/or carrier mobility in GBMs. When used synergistically, they ensure comprehensive material evaluation while balancing efficiency, accuracy, and application needs. This is exemplified by Buron et al., who combined micro four-point probe (M4PP) and THz-TDS to quantitatively map sheet conductance uniformity in large-area CVD graphene (Fig. 13c)[69].

7 Conclusions and prospects

Eighteen measurement standards for characterizing six critical characteristics, such as number of layers, defects, functional groups, elemental composition, sheet resistance, and carrier mobility, of GBMs are systematically examined. For each characteristic, this review comprehensively analyzes available international standards, exploring applicable sample types, fundamental principles of adopted techniques, and specific precautions. Notably, experimental details (e.g., calibration, procedures, data analysis) are excluded. Users should consult original standards for specific guidance. A decision-making framework (Fig. 14) provides structured guidance for rapid standard selection, enabling industry and academia to identify optimal standards for their applications. This general review anticipates more detailed guides as research progresses. Enforcement of these standards is pivotal for enhancing GBMs' commercial value. A transparent market ecosystem, built on collective adherence of robust standards by producers, buyers, and researchers, ensures equitable benefits and fosters full-fledged support for GBMs development and commercialization.

Notwithstanding significant progress, future research must prioritize the following issues to bridge the current gap in developing and implementing robust measurement standards for GBMs. Firstly, ad-

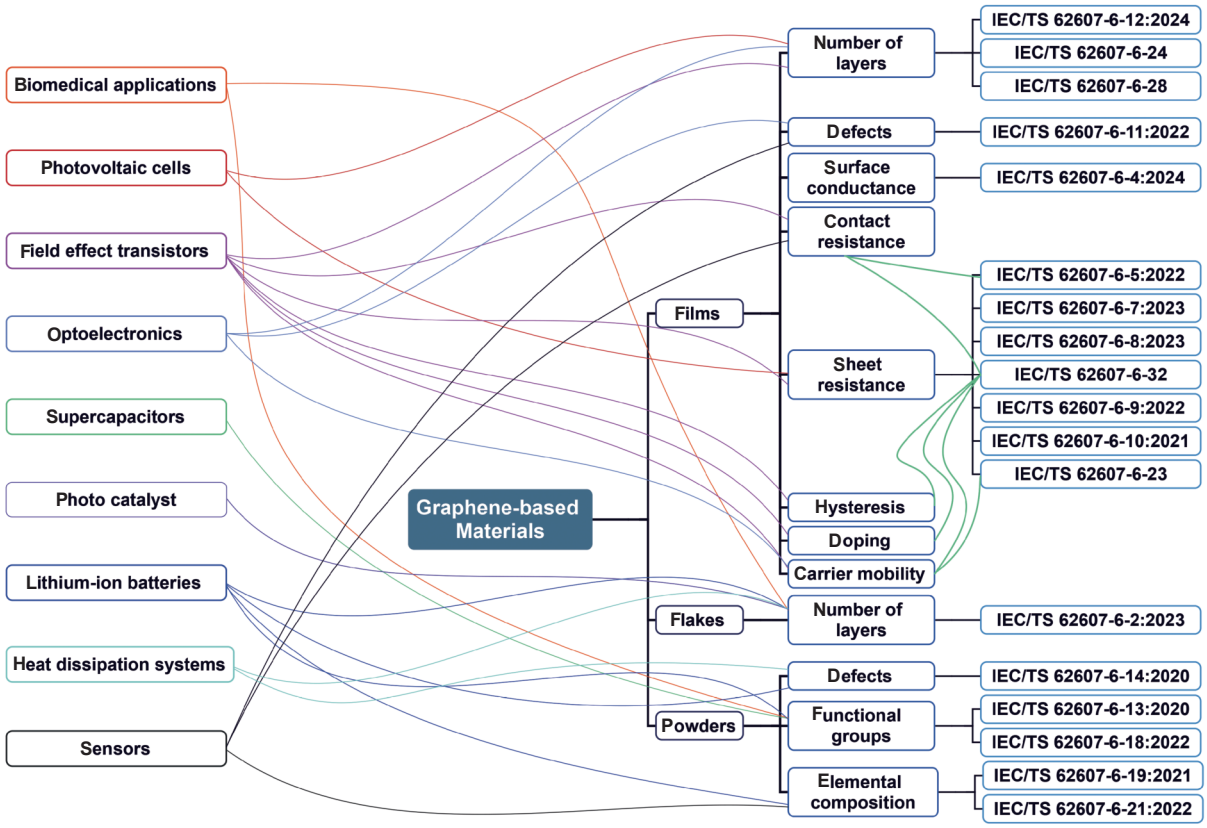

Fig. 14 Decision framework for different forms of graphene-based materials

vanced characterization techniques, despite their high precision in material analysis, remain scarcely adopted industrially. High-end instruments involve exorbitant purchasing and maintenance cost. Additionally, their operation is complex and requires highly specialized skills. These factors restrict accessibility, particularly for small and medium-sized enterprises. Standards based on cost-effective alternative techniques ensuring comparable accuracy and reliability should be promoted. Secondly, prevalent standardization discrepancies impede the global trade and fragment the GBMs market. Round-robin intercomparisons highly recommended in ISO frameworks should be integrated into standard development. These intercomparisons serve multiple purposes: assessing cross-scenario reliability to reduce regional fragmentation, evaluating technical reproducibility and operational viability, enhancing global data comparability for international trade. Last but not the least, the deepening of industrial applications and the advancement of academic frontiers have given rise to new demands for measurement standards. For instance, in electronics and energy storage applications, graphene slurry requires standards for critical manufacturing traits. These incldes dispersion, shelf life, and resistance to re-agglomeration, for which established protocols are currently lacking. Concurrently, biomedical research on graphene drives demands for new standards addressing parameters like surface chemistry regulation, cytotoxicity assessment, and protein binding capacity in complex biological systems.

Acknowledgements

This work was supported by the National Key Research and Development (R&D) Program of China (2022YFF0609801) and the Science and Technology Project of Special Equipment Safety Supervision Inspection Institute of Jiangsu Province (KJ(Y) 2023053).

References

[1] Yang Z, Gao R G, Hu N T, et al. The prospective two-dimensional graphene nanosheets: preparation, functionalization, and applications[J]. Nano-Micro Letters, 2012, 4(1): 1-9.

[2] Gutiérrez-Cruz A, Ruiz-Hernández A R, Vega-Clemente J F, et al. A review of top-down and bottom-up synthesis methods for the production of graphene, graphene oxide and reduced graphene oxide[J]. Journal of Materials Science, 2022, 57: 14543-14578.

[3] Zhu Y W, Murali S, Cai W W, et al. Graphene and graphene oxide: synthesis, properties, and applications[J]. Advanced Materials, 2010, 22: 3906-3924.

[4] Olabi A G, Abdelkareem M A, Wilberforce T, et al. Application of graphene in energy storage device – A review[J]. Renewable Sustainable Energy Reviews, 2021, 135: 110026.

[5] Razaq A, Bibi F, Zheng X X, et al. Review on graphene-, graphene oxide-, reduced graphene oxide-based flexible composites: from fabrication to applications[J]. Materials, 2022, 15: 1012.

[6] Kauling A P, Seefeldt A T, Pisoni D P, et al. The worldwide graphene flake production[J]. Advanced Materials, 2018, 30: 1803784.

[7] Bøggild P. Research on scalable graphene faces a reproducibility gap[J]. Nature Communications, 2023, 14: 1126.

[8] Bøggild P. The war on fake graphene[J]. Nature, 2018, 562: 502-503.

[9] Liu M Y, Wang L P, Yu G. Recent research progress of porous graphene and applications in molecular sieve, sensor, and supercapacitor[J]. Small, 2024, 20: 2401767.

[10] Yang Y, Wei Y H, Guo Z F, et al. From materials to devices: graphene toward practical applications[J]. Small Methods, 2022, 6: 2200671.

[11] Li H-L, Xiao S-N, Yu H-L, et al. A review of graphene-based films for heat dissipation[J]. New Carbon Materials, 2021, 36(5): 897-910.

[12] Alves T, Mota W S, Barros C, et al. Review of scientific literature and standard guidelines for the characterization of graphene-based materials[J]. Journal of Materials Science, 2024, 59: 14948-14980.

[13] Pollard A J. Metrology for graphene and 2D materials[J]. Measurement Science and Technology, 2016, 27: 092001.

[14] ISO, ISO/TS 21356-1: 2021 Nanotechnologies — Structural characterization of graphene — Part 1: Graphene from powders and dispersions (S). 2021[2025-4-24]. https://www.iso.org/standard/70757.html.

[15] ISO, ISO/TR 19733: 2019 Nanotechnologies — Matrix of properties and measurement techniques for graphene and related two-dimensional (2D) materials (S). 2019[2025-4-24]. https://www.iso.org/standard/66188.html?browse=tc.

[16] Cao M H, Su J, Fan S Q, et al. Wearable piezoresistive pressure sensors based on 3D graphene[J]. Chemical Engineering Journal, 2021, 406: 126777.

[17] Ji L W, Meduri P, Agubra V, et al. Graphene-based nanocomposites for energy storage[J]. Advanced Energy Materials, 2016, 6: 1502159.

[18] Nargatti K I, Pathak T S, Ahankari S S, et al. Graphene-based inks for flexible supercapacitor electrodes: A review[J]. ACS Applied Electronic Materials, 2024, 6: 24-46.

[19] Xu S C, Wang S S, Chen Z, et al. Electric-field-assisted growth of vertical graphene arrays and the application in thermal interface materials[J]. Advanced Functional Materials, 2020, 30: 2003302.

[20] Yan H, Wang Q, Wang J Y, et al. Planted graphene quantum dots for targeted, enhanced tumor imaging and long-term visualization of local pharmacokinetics[J]. Advanced Materials, 2023, 35: 2210809.

[21] Béraud A, Sauvage M, Bazán C M, et al. Graphene field-effect transistors as bioanalytical sensors: design, operation and performance[J]. Analyst, 2021, 146: 403.

[22] Kumar V, Kumar A, Lee D-J, et al. Estimation of number of graphene layers using different methods: A focused review[J]. Materials, 2021, 14: 4590.

[23] Du Y N, Wang M Y, Ye X L, et al. Advances in the field of graphene-based composites for energy-storage applications[J]. Crystals, 2023, 13: 912.

[24] Hwangbo Y, Lee C-K, Mag-Isa A E, et al. Interlayer non-coupled optical properties for determining the number of layers in arbitrarily stacked multilayer graphenes[J]. Carbon, 2014, 77: 454-461.

[25] Prakash G, Capano M A, Bolen M L, et al. AFM study of ridges in few-layer epitaxial graphene grown on the carbon-face of 4H–SiC(000$\bar{1}$)[J]. Carbon, 2010, 48: 2383-2393.

[26] Ferrari A C, Basko D M. Raman spectroscopy as a versatile tool for studying the properties of graphene[J]. Nature Nanotechnolgy, 2013, 8: 235-246.

[27] IEC, IEC/TS 62607-6-12: 2024 Nanomanufacturing – Key control characteristics – Part 6-12: Graphene – Number of layers: Raman spectroscopy, optical reflection (S). 2024[2025-4-24]. https://www.iec.ch/dyn/www/f?p=103:38:400224410772319::::FSP_ORG_ID,FSP_APEX_PAGE,FSP_PROJECT_ID:1315,20,104930.

[28] IEC, IEC/TS 62607-6-2: 2023 Nanomanufacturing – Key control characteristics – Part 6-2: Graphene – Number of layers: atomic force microscopy, optical transmission, Raman spectroscopy (S). 2023[2025-4-24]. https://www.iec.ch/dyn/www/f?p=103:38:400224410772319::::FSP_ORG_ID,FSP_APEX_PAGE,FSP_PROJECT_ID:1315,20,21465.

[29] Ni Z H, Wang H M, Kasim J, et al. Graphene thickness determination using reflection and contrast spectroscopy[J]. Nano Letters, 2007, 7: 2758-2763.

[30] IEC, IEC/TS 62607-6-24 Nanomanufacturing – Key control characteristics – Part 6-24: Graphene-related products – Number of layer distribution of graphene films: Optical contrast method (S). under development[2025-4-24]. https://www.iec.ch/dyn/www/f?p=103:38:400224410772319::::FSP_ORG_ID,FSP_APEX_PAGE,FSP_PROJECT_ID:1315,20,102646.

[31] IEC, IEC/TS 62607-6-28 Nanomanufacturing – Key control characteristics – Part 6-28: Graphene-related products – Number of layers for graphene films on a substrate: Raman spectroscopy (S). under development[2025-4-24]. https://www.iec.ch/dyn/www/f?p=103:38:400224410772319::::FSP_ORG_ID,FSP_APEX_PAGE,FSP_PROJECT_ID:1315,20,104937.

[32] Wang B, Ruan T T, Chen Y, et al. Graphene-based composites for electrochemical energy storage[J]. Energy Storage Materials, 2020, 24: 22-51.

[33] Liu H P, Lei W, Tong Z M, et al. Defect engineering of 2D materials for electrochemical energy storage[J]. Advanced Materials Interfaces, 2020, 7: 2000494.

[34] Khossossi N, Singh D, Ainane A, et al. Recent progress of defect chemistry on 2D materials for advanced battery anodes[J]. Chemistry-An Asian Journal, 2020, 15: 3390-3404.

[35] Zhang H W, Lv R T. Defect engineering of two-dimensional materials for efficient electrocatalysis[J]. Journal of Materiomics, 2018, 4: 95-107.

[36] Yuan R L, Wang H H, Shang L, et al. Revealing the self-doping defects in carbon materials for the compact capacitive energy storage of Zn-ion capacitors[J]. ACS Applied Materials & Interfaces, 2023, 15: 3006-3016.

[37] IEC, IEC/TS 62607-6-14: 2020 Nanomanufacturing – Key control characteristics – Part 6-14: Graphene-based material – Defect level: Raman spectroscopy (S). 2020[2025-4-24]. https://www.iec.ch/dyn/www/f?p=103:38:400224410772319::::FSP_ORG_ID,FSP_APEX_PAGE,FSP_PROJECT_ID:1315,20,23868.

[38] IEC, IEC/TS 62607-6-11: 2022 Nanomanufacturing – Key control characteristics – Part 6-11: Graphene – Defect density: Raman spectroscopy (S). 2022[2025-4-24]. https://www.iec.ch/dyn/www/f?p=103:38:400224410772319::::FSP_ORG_ID,FSP_APEX_PAGE,FSP_PROJECT_ID:1315,20,23866.

[39] Cançado L G, Monken V P, Campos J L E, et al. Science and metrology of defects in graphene using raman spectroscopy[J]. Carbon, 2024, 220: 118801.

[40] Muller D A, Mills M J. Electron microscopy: probing the atomic structure and chemistry of grain boundaries, interfaces and defects[J]. Materials Science and Engineering A-Structural Materials Properties Microstructure and Processing, 1999, 260: 12-28.

[41] Liang X Y, Ng S-P, Ding N, et al. Characterization of point defects in monolayer arsenene[J]. Applied Surface Science, 2018, 443: 74-82.

[42] Stergiou A, Cantón-Vitoria R, Psarrou M N, et al. Functionalized graphene and targeted applications – highlighting the road from chemistry to applications[J]. Progress in Materials Science, 2020, 114: 100683.

[43] Sturala J, Luxa J, Pumera M, et al. Chemistry of graphene derivatives: synthesis, applications, and perspectives[J]. Chemistry-A European Journal, 2018, 24: 5992-6006.

[44] IEC, IEC/TS 62607-6-18: 2022 Nanomanufacturing – Key control

characteristics – Part 6-18: Graphene-based material – Graphene-based material – Functional groups: TGA-FTIR (S). 2022[2025-4-24]. https://www.iec.ch/dyn/www/f?p=103:38:400224410772319:::FSP_ORG_ID,FSP_APEX_PAGE,FSP_PROJECT_ID:1315,20,101668.

[45] IEC, IEC/TS 62607-6-13: 2020 Nanomanufacturing – Key control characteristics – Part 6-13: Graphene-based material – Oxygen functional group content: Boehm titration method (S). 2020[2025-4-24]. https://www.iec.ch/dyn/www/f?p=103:38:400224410772319:::FSP_ORG_ID,FSP_APEX_PAGE,FSP_PROJECT_ID:1315,20,23867.

[46] Aliyev E, Filiz V, Khan M M, et al. Structural characterization of graphene oxide: surface functional groups and fractionated oxidative debris[J]. Nanomaterials, 2019, 9: 1180.

[47] Skripov A V, Soloninin A V, Valeeva A A, et al. Hydrogen in nonstoichiometric cubic titanium monoxides: X-ray and neutron diffraction, neutron vibrational spectroscopy and NMR studies[J]. Journal of Alloy and Compounds, 2021, 887: 161353.

[48] Humeres E, Aliev A E, Smaniotto A, et al. Intramolecular amino-thiolysis cyclization of graphene oxide modified with sulfur dioxide: XPS and solid-state NMR studies[J]. Journal of Physical Chemistry C, 2022, 126: 1729-1741.

[49] Mali K S, Greenwood J, Adisoejoso J, et al. Nanostructuring graphene for controlled and reproducible functionalization[J]. Nanoscale, 2015, 7: 1566-1585.

[50] Zhou Y-C, Zhang H-L, Deng W-Q. A 3*N* rule for the electronic properties of doped graphene[J]. Nanotechnology, 2013, 24: 225705.

[51] IEC, IEC/TS 62607-6-19: 2021 Nanomanufacturing – Key control characteristics – Part 6-19: Graphene-based material – Elemental composition: CS analyser, ONH analyser (S). 2021[2025-4-24]. https://www.iec.ch/dyn/www/f?p=103:38:400224410772319:::FSP_ORG_ID,FSP_APEX_PAGE,FSP_PROJECT_ID:1315,20,101669.

[52] IEC, IEC/TS 62607-6-21: 2022 Nanomanufacturing – Key control characteristics – Part 6-21: Graphene-based material – Elemental composition, C/O ratio: X-ray photoelectron spectroscopy (S). 2022[2025-4-24].https://www.iec.ch/dyn/www/f?p=103:38:400224410772319:::FSP_ORG_ID,FSP_APEX_PAGE,FSP_PROJECT_ID:1315,20,101672.

[53] ISO, ISO/TS 13278: 2017 Nanotechnologies — Determination of elemental impurities in samples of carbon nanotubes using inductively coupled plasma mass spectrometry (S). 2017[2025-4-24]. https://www.iso.org/standard/69310.html?browse=tc.

[54] Yusaf T, Mahamude A S F, Farhana K, et al. A Comprehensive review on graphene nanoparticles: preparation, properties, and applications[J]. Sustainability, 2022, 14: 12336.

[55] IEC, IEC/TS 62607-6-7: 2023 Nanomanufacturing-Key control characteristics – Part 6-7: Graphene – Sheet resistance: van der Pauw method (S). 2023[2025-4-24]. https://www.iec.ch/dyn/www/f?p=103:38:400224410772319:::FSP_ORG_ID,FSP_APEX_PAGE,FSP_PROJECT_ID:1315,20,104304.

[56] Zhang H H, Mischke J, Mertin W, et al. Graphene as a transparent conductive electrode in GaN-based LEDs[J]. Materials, 2022, 15: 2203.

[57] Chandramohan S, Ko K B, Yang J H, et al. Performance evaluation of GaN light-emitting diodes using transferred graphene as current spreading layer[J]. Journal of Applied Physics, 2014, 115: 054503.

[58] IEC, IEC/TS 62607-6-8: 2023 Nanomanufacturing – Key control characteristics – Part 6-8: Graphene – Sheet resistance: In-line four-point probe (S). 2023[2025-4-24]. https://www.iec.ch/dyn/www/f?p=103:38:400224410772319:::FSP_ORG_ID,FSP_APEX_PAGE,FSP_PROJECT_ID:1315,20,23863.

[59] Cultrera A, Serazio D, Fabricius N, et al. New IEC standards for the measurement of sheet resistance on large-area graphene using the van der Pauw and the in-line four-point probe methods[J]. Measurement, 2024, 236: 114980.

[60] IEC, IEC/TS 62607-6-5: 2022 Nanomanufacturing – Key control characteristics – Part 6-5: Graphene-based materials – Contact resistance and sheet resistance: transmission line measurement (S). 2022[2025-4-24]. https://www.iec.ch/dyn/www/f?p=103:38:400224410772319:::FSP_ORG_ID,FSP_APEX_PAGE,FSP_PROJECT_ID:1315,20,23442.

[61] Quellmalz A, Smith A D, Elgammal K, et al. Influence of humidity on contact resistance in graphene devices[J]. ACS Applied Materials & Interfaces, 2018, 10: 41738-41746.

[62] Watanabe E, Conwill A, Tsuya D, et al. Low contact resistance metals for graphene based devices[J]. Diamond and Related Materials, 2012, 24: 171-174.

[63] IEC, IEC/TS 62607-6-9: 2022 Nanomanufacturing – Key control characteristics – Part 6-9: Graphene-based material – Sheet resistance: Eddy current method (S). 2022[2025-4-24]. https://www.iec.ch/dyn/www/f?p=103:38:400224410772319:::FSP_ORG_ID,FSP_APEX_PAGE,FSP_PROJECT_ID:1315,20,23864.

[64] IEC, IEC/TS 62607-6-10: 2021 Nanomanufacturing – Key control characteristics – Part 6-10: Graphene-based material – Sheet resistance: Terahertz time-domain spectroscopy (S). 2021[2025-4-24]. https://www.iec.ch/dyn/www/f?p=103:38:400224410772319:::FSP_ORG_ID,FSP_APEX_PAGE,FSP_PROJECT_ID:1315,20,23865.

[65] IEC, IEC/TS 62607-6-4: 2024 Nanomanufacturing-Key control characteristics- Part 6-4: Graphene-based materials-Surface conductance: non-contact microwave resonant cavity method (S). 2024[2025-4-24]. https://www.iec.ch/dyn/www/f?p=103:38:400224410772319:::FSP_ORG_ID,FSP_APEX_PAGE,FSP_PROJECT_ID:1315,20,104984.

[66] Catanzaro A, Huang N J, Melios C, et al. Good practice guide on the electrical characterization of graphene using non-contact and high-throughput methods[EB/OL].[2025-6-30]. http://empir.npl.co.uk/grace/.

[67] IEC, IEC/TS 62607-6-32 Nanomanufacturing – Key control characteristics – Part 6-32: Two-dimensional materials – Charge carrier mobility, contact resistance, sheet resistance, doping, and hysteresis: Gated transfer length method (S). under development[2025-4-24]. https://www.iec.ch/dyn/www/f?p=103:

38:400224410772319::::FSP_ORG_ID,FSP_APEX_PAGE,FSP_PROJECT_ID:1315,20,108113.

[68] IEC, IEC/TS 62607-6-23 Nanomanufacturing – Key control characteristics – Part 6-23: Graphene film – Carrier Mobility and Sheet Resistance: Hall measurement (S). under development[2025-4-24]. https://www.iec.ch/dyn/www/f?p=103:38:400224410772319::::FSP_ORG_ID,FSP_APEX_PAGE,FSP_PROJECT_ID:1315,20,102645.

[69] Buron J D, Petersen D H, Bøggild P, et al. Graphene conductance uniformity mapping[J]. Nano Letters, 2012, 12: 5074-5081.